JOURNAL OF OPTOELECTRONICS AND ADVANCED MATERIALS Vol. 10, No. 4, April 2008, p. 750 - 756

Invited Paper

High energy permanent magnets

E. BURZO*, P. VLAIC
Faculty of Physics, Babes-Bolyai University Cluj-Napoca, Romania

Band structure calculations were performed on $R_2Fe_{14}B$, $R_2Fe_{14}C$, $R_2Co_{14}B$, R_2Fe_{17} and R_2Co_{17} compounds, where R is a rare earth. The exchange interactions in these systems are discussed in 4f-5d-3d model. Then, we analyse the magnetic properties of Nd-Fe-Si-B and Sm-Fe-Si-C permanent magnets. The magnetocaloric effect in Nd-Fe-Si-B is also estimated. The effects of Fe substitutions by (Co+Al) on the Curie temperatures and anisotropy fields of the hard magnetic phases $R_2Fe_{14}B$ (R = Pr,Nd) are presented. Finally, the permanent magnet properties of $Sm(Co,Fe,Cu,Zr)_z$ alloys are analysed in correlation with composition and annealing treatments.

(Received February 25, 2008; accepted April 2, 2008)

Keywords: Rare earth magnets, Band structures, Magnetocaloric effect, Exchange interactions

1. Introduction

The rare-earth(R)-transition metal (M = Co,Fe) compounds are of great interest for technical applications, particularly in manufacturing permanent magnets. The rare-earth-cobalt permanent magnets are based on RCo_5 or R_2Co_{17}-type compounds. The high Curie temperatures, T_c, of these systems are mainly determined by the contribution of cobalt sublattice to exchange interactions. Since for light rare-earths, the magnetic moments are parallely oriented to those of cobalt, high saturation magnetizations were evidenced [1]. Thus, for the use as permanent magnet materials, the Sm-Co alloys were considered, since as cobalt atoms, Sm ones show uniaxial anisotropy in both $SmCo_5$ and Sm_2Co_{17} systems.

The R_2Fe_{17} compounds have low Curie temperatures, the highest one, T_c = 477 K, was evidenced for R=Gd. Somewhat higher temperatures, around 600 K, were found in $R_2Fe_{14}B$ and $R_2Fe_{14}C$ systems [2]. The above mentioned values are about half of the Curie temperature of pure iron, although the iron content in these compounds is 90 at % and 82 at %, respectively. In both systems, the mean iron moments are close to that of pure iron. Due to the low T_c values and planar anisotropies, the R_2Fe_{17} compounds have been considered as not useful for technical applications, such as permanent magnets. In spite of the relatively low Curie points, the R-Fe-B magnets, based on $R_2Fe_{14}B$ phases, have excellent properties at room temperature. Researches were directed to improve their performances at higher temperatures. From an economical point of view, the Nd-Fe-B magnets have a price advantage over the Sm-Co ones, due to more abundance of the raw materials.

In this paper we analyse, in the first part, the exchange interactions in rare-earth transition metal compounds having possible applications as permanent magnets. Accordingly, band structure calculations were performed. Then, we discuss some ways to improve the performances of permanent magnets. In this context we analyse the magnetic properties of some alloys as Nd-Fe-Si-B, Nd-Fe-Co-Al-B, Sm-Fe-Si-C and $Sm(Co,Fe,Cu,Zr)_z$.

2. Exchange interactions in R–M and R–M–B type compounds

The exchange interactions in R-M and R-M-B compounds, between rare-earth and transition metals, can be described by the 4f-5d-3d model [3]. In this model, the 4f moment of R atom induces a positive local 5d spin moment through the ordinary intra-atomic 4f-5d or 4f-6s exchange with subsequent direct 5d-nd exchange interactions with other nd shells of neighbouring atoms. The 4f-5d exchange interactions are dominant. There are also short range interactions between M atoms.

The exchange interactions between iron atoms in R_2Fe_{17} and $R_2Fe_{14}B$ compounds are rather complex. In both $P6_3/mmc$ and $R\bar{3}m$ type structures, in which crystallize R_2Fe_{17} compounds, iron is distributed in four lattice sites. The tetragonal $P4_2/mmm$ lattice of $R_2Fe_{14}A$ (A = B,C) compounds has 6 different iron lattice sites. For a given site, the distances between iron atoms cover a large range of values. The interactions between iron atoms situated at distances $d_{Fe\text{-}Fe} \leq 2.50$ Å are negative. Values of 2.39 Å and 2.44 Å were evidenced between $Fe(j_1)$–$Fe(k_2)$ and $Fe(j_1)$–$Fe(j_1)$ atoms, respectively, in $Nd_2Fe_{14}B$ compound. A similar situation was shown in R_2Fe_{17} compounds, where the distances between Fe(f)-Fe(f), Fe(g)-Fe(k), Fe(g)-Fe(j) and Fe(k)-Fe(k) are smaller than 2.50 Å [4]. Since interactions with iron atoms, situated at greater distances than 2.50 Å, are positive and stronger, than the negative ones, the last ones are not satisfied. Consequently, a large magnetic energy is stored. This brings about the low magnetic ordering temperatures of R_2Fe_{17} and $R_2Fe_{14}A$ (A = B,C) compounds. The presence of interstitial atoms in the above structures increases the lattice constants diminishing or canceling the negative exchange interactions, thus increasing the Curie temperatures. A similar effect can be obtained by substituting iron atoms in sites involved in negative exchange interactions.

In order to analyse the exchange interactions in $R_2Fe_{14}B$, $R_2Fe_{14}C$, $R_2Co_{14}B$, R_2Fe_{17} and R_2Co_{17} compounds, band structure calculations were performed. We note that there were published some such calculations on the above systems [2,5].

Band structure calculations were performed by using the ab initio tight binding linear muffin tin orbital method, in the atomic sphere approximation (TB-LMTO-ASA) [6]. In the framework of the local density approximation (LDA), the total electronic potential is the sum of external, Coulomb and exchange correlation energies [7]. The functional form of the exchange correlation energy, used in the present work, was the free electron gas parameterization of Von-Barth and Hedin [8]. Relativistic effects were included. The 4f states were treated as part of the band structure, but the polarization of the 4f densities was calculated self-consistently.

The computed iron moments in $R_2Fe_{14}B$, $R_2Fe_{14}C$ and $R_2Fe_{14}B$ compounds are given in Figs. 1-3, as function of De Gennes factor, $G = (g_J-1)^2J(J+1)$. In Fig.4 are plotted the values of the iron moments determined in R_2Fe_{17} compounds and in Fig. 5 those of cobalt calculated in R_2Co_{17} system with heavy rare-earths. In all cases linear relations, M_M vs. G were shown, described by:

$$M_M = M_M(0) + \alpha G \quad \text{with M = Fe,Co} \qquad (1)$$

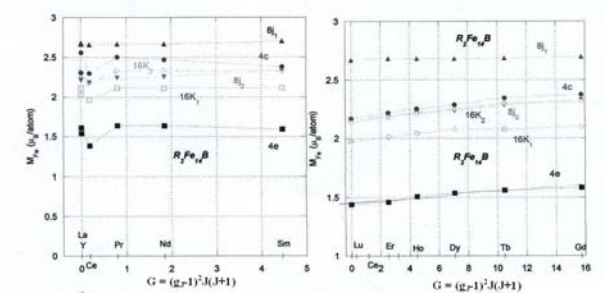

Fig. 1. Computed iron moments in $R_2Fe_{14}B$ compounds as function De Gennes factor, $G = (g_J-1)^2J(J+1)$.

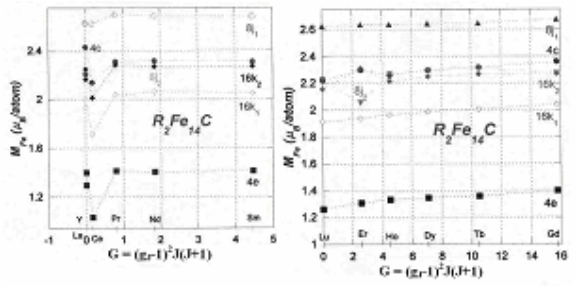

Fig. 2. Computed iron moments in $R_2Fe_{14}C$ compounds as function of De Gennes factor.

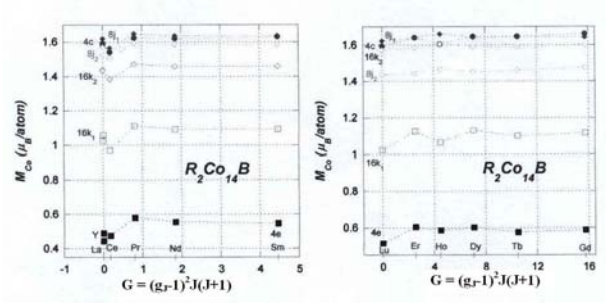

Fig. 3. Cobalt moments in $R_2Co_{14}B$ compounds.

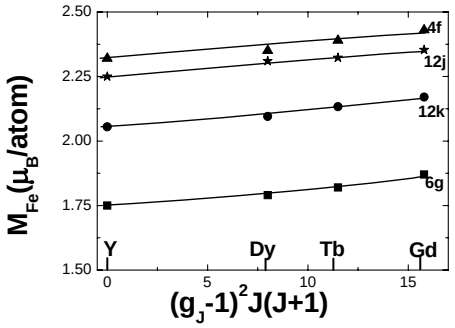

Fig. 4. Iron moments in hexagonal R_2Fe_{17} heavy rare-earth and yttrium compounds.

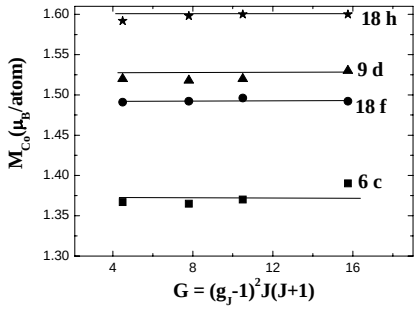

Fig. 5. Cobalt moments in R_2Co_{17} compounds with heavy rare-earths.

We denoted by $M_M(0)$, the magnetic moments of transition metals characteristic at G = 0 and α describes the slopes of these dependences.

From the above trend, the cerium compounds deviate. This can be correlated with the valence state of cerium, more close to +4 than from +3, generally characteristic for other rare-earths. The Ce 4f states are not localized and a hybridization with Fe and Co 3d states takes place.

The variation of iron moments in $R_2Fe_{14}B$ and $R_2Fe_{14}C$ compounds can be described by a value $\alpha=5\cdot10^{-2}\mu_B$, while in R_2Fe_{17} a slope $\alpha=4\cdot10^{-2}\mu_B$ was obtained. Thus, a fraction of 5-8 % of the iron moments is induced by 4f-5d-3d exchange interactions when replacing a nonmagnetic rare-earth or yttrium by magnetic ones. These data show that iron has no a great degree of itinerancy. The analyses of these data show that iron moments are dependent of their local environments. As example, in $Y_2Fe_{14}B$, where Y has no magnetic moment, the largest M_{Fe} value was determined on the j_1 site having an iron coordination 12 out of 14. On the other hand, the iron moment is reduced on 4c sites with the highest Y coordination, 4 out 8 [9]. The mean iron moments in the $R_2Fe_{14}A$ and R_2Fe_{14} compounds are situated between 2.15 and 2.22 μ_B, close to the value determined in pure iron.

When considering only spin contributions, the sequence in decreasing the iron moment can be somewhat changed. As example in R_2Fe_{17} compounds, when both spin and orbital contributions were considered we have M(f) > M(j) > M(k) > M(g). When only spin contribution was

taken into account, in the above sequence, the M(f) and M(j) moments were inverted.

In order to obtain more information on the degree of itinerancy of iron moments, paramagnetic measurements were performed [10-12]. In $R_2Fe_{14}B$ and R_2Fe_{17} compounds a mean effective moment of $\cong 4.0\ \mu_B$/atom was determined. The ratio between the mean number of spins determined from effective moments, S_p, and that obtained from saturation measurements, S_o, $r = S_p/S_o$ is 1.24(7). This value indicates no high degree of itinerancy, in agreement with the variation of iron moments as function of R partner.

The cobalt moments both in $R_2Co_{14}B$ and R_2Co_{17} compounds are very little dependent on composition. In addition, in R_2Co_{17} series, the mean cobalt moments are only by $0.1\mu_B$ little smaller than of the pure cobalt. This difference is greatest in $R_2Co_{14}B$ compounds, namely $\cong$ 0.30 μ_B. The little variation of cobalt moments with rare-earth partner can be correlated with the relative small contributions of the 4f-5d-3d exchange interactions as compared to those between cobalt atoms. This is confirmed also by small variations of Curie temperatures along the series.

The R5d band polarizations in R_2M_{17} (M=Fe,Co,Ni) – Fig.6 – as well as in $R_2Fe_{14}B$ compounds follow also linear dependences as function of De-Gennes factor:

$$M_{5d} = M_{5d}(0) + \beta G \qquad (2)$$

The M_{5d} band polarizations have the same dependences with $\beta \cong 1\cdot10^{-2}\mu_B$, but are translated at higher values as the magnetizations of transition metals, corresponding to one R atom are greater. For $P6_3/mmc$ type structure of R_2Fe_{17} compounds, where two R sites are present (2b and 2d), the M_{5d} values are only slightly different. A higher difference between M_{5d} band polarizations at R(4f) and R(4g) sites can be seen in $R_2Fe_{14}B$ compounds. The observed difference can be correlated with their different local environments, the R(4g) site having a higher number of boron atoms in the first coordination shell. In Fig.6, the corresponding mean values are plotted.

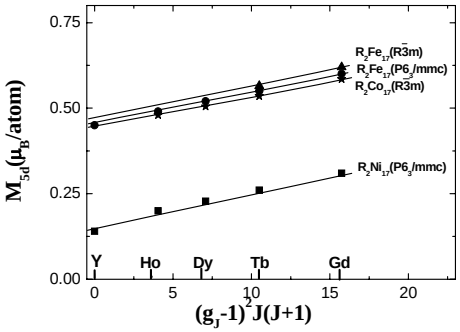

Fig. 6. Rare-earth 5d band polarizations in R_2M_{17} (M = Fe,Co,Ni) heavy rare earth compound. The Y4d band polarizations in Y_2Ni_{17}, Y_2Fe_{17} and $Y_2Fe_{14}B$ are also plotted.

The analyses of the data from Fig.6 show the presence of two contributions to R5d band polarizations. The βG term is due to intra-atomic 4f-5d exchange and is the same for a given R atom, independent on M partener. The $M_{5d}(0)$ values can be ascribed to the induced polarizations due to short range 5d-nd exchange interactions with neighbouring atoms. These interactions can be described by the Hamiltonian [13].

$$H = -2J_{3d-5d}S_{5d}(0)\sum_i S_{3d_i}(0) - 2J_{5d-5d}S_{5d}(0)\sum S_{5d_j} \qquad (3)$$

We denoted by $J_{3d\text{-}5d}$ and $J_{5d\text{-}5d}$ the exchange parameters characterizing the 3d-5d and 5d-5d interactions with i and j nearest neighbours M and R atoms, respectively. The $S_{5d}(0)$ and $S_{3d}(0)$ are the spin values corresponding to G = 0, with nonmagnetic rare-earth, respectively.

The relation (3) can be analysed in the molecular field approximation. The effect of 5d-3d and 5d-5d exchange interactions is equivalent to an effective field, H_{exch}, acting on R atom. This induces an additional 5d polarization to that resulting from intra-atomic 4f-5d exchange. This situation is similar to that evidenced in R-M compounds, where an additional 3d magnetic moment is induced by the exchange field [14]. The 3d induced moments were shown to be linearly dependent on the exchange fields.

We assume, in a first approximation, that $J_{5d\text{-}3d} \cong J_{5d\text{-}5d}$. Taking into account that $M_{5d} \propto H_{exch}$, as suggested by relation (3) and that $M_{nd} \propto H_{exch}$, it follows that $M_{5d}(0) = \gamma M_d$.

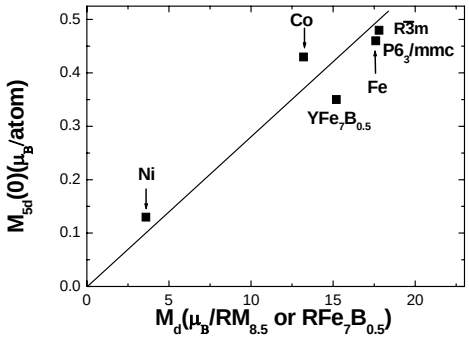

Fig. 7. The $M_{5d}(0)$ contributions to 5d or 4d band polarizations as function of transition metal moments in $RM_{8.5}$ (M =Fe,Co,Ni) and the mean polarizations of R5d or Y4d bands in $RM_7B_{0.5}$ (half of unit formula were considered).

The $M_{5d}(0)$ values determined in $RM_{8.5}$ and the mean values obtained in $RFe_7B_{0.5}$ compounds are plotted in Fig.7 as function of M_d magnetizations. The data suggested a linear dependence, in agreement with the above conclusion. The determined slope is $(2.8 \pm 0.4)\cdot10^{-2}$. Comparing these data with the induced M moments in R-Co and R-Fe compounds we concluded that the polarizations of R5d bands are more sensitive to exchange interactions than those of the Fe3d band and of the same order of magnitude as on cobalt in RCo_2 compounds.

3. Nd-Fe-Si-B permanent magnets

The effect of iron substitution by silicon on the magnetic properties of Nd-Fe-B magnets will be analysed. A favorable effect was suggested by the analyses of the composition dependences of the Curie temperatures of hard magnetic phase [2] as well as of anisotropy field – Fig. 8. For a small quantity of Fe substituted by Si (x = 0.5) the anisotropy field increases by 15 %.

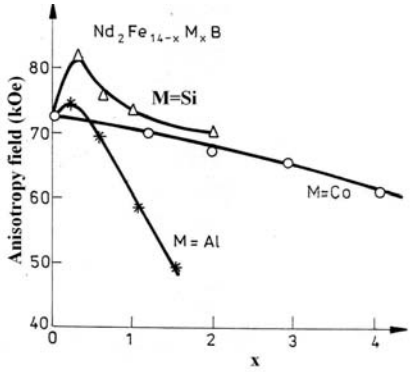

Fig. 8. Composition dependences of the anisotropy fields in $Nd_2Fe_{14-x}M_xB$ with M = Si, Al and Co.

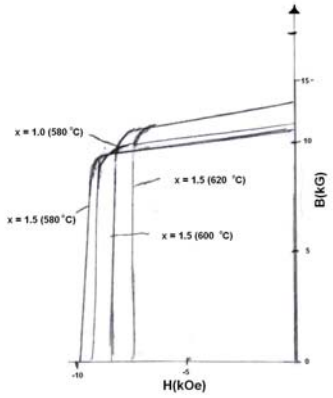

Fig. 9. Demagnetizing curves for some $Nd_{15}Fe_{77-y}Si_yB_8$ magnets.

The $Nd_{15}Fe_{77-y}Si_yB_8$ with $x \leq 3$ were prepared by melting the constituent elements in an induction furnace. The samples were crushed and milled to 1-2 μm mean grain size. The samples were aligned in a magnetic field of 30 kOe and pressed. Then, these were sintered at 1080 ^oC during 1 h and then thermally treated at temperatures between 580-630 ^oC during 0.5 h. The best technical parameters were obtained by thermal treatment at 590 ^oC. Some demagnetization curves are shown in Fig.9, evidencing the influence of composition and thermal treatment on remanent induction, B_r and coercive field, H_C.

The evolution of coercive field, at room temperature, as function of silicon content is shown in Fig. 10. A continous increase in H_c values was evidenced. This can be correlated both with increasing of the anisotropy fields as well as of Curie temperatures. A composition of $Nd_{15}Fe_{77-y}Si_yB$ with y = 2.0, corresponds to 0.4 Fe atoms substituted by Si in the hard magnetic phase, where the anisotropy was shown to be increased.

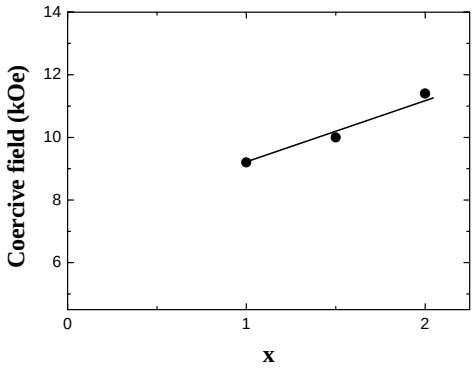

Fig. 10. Composition dependence of the coercive fields in $Nd_{15}Fe_{76}SiB_8$ magnets.

The temperature dependences of the coercive fields in $Nd_{15}Fe_{76}Si_1B_8$ and $Nd_{15}Fe_{75}Si_2B_8$ magnets are shown in Fig. 11. The coercive fields are somewhat greater in silicon doped samples with x = 2 and have a more little decrease with temperature than for the $Nd_{15}Fe_{76}Si_1B_8$ magnet. The energy products varied between 19 and 35 MGOe.

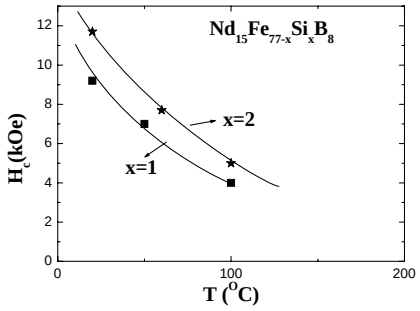

Fig. 11. Temperature dependences of the coercive fields in $Nd_{15}Fe_{76}SiB_8$ and $Nd_{15}Fe_{75}Si_2B_8$ alloys.

The magnetocaloric effect was determined in the $Nd_{15}Fe_{76}Si_1B_8$ alloy starting from magnetization isotherms. The entropy change, ΔS_M, was determined from the following relation:

$$\Delta S_M = \sum_i \frac{1}{T_{i+1} - T_i} (M_{i+1} - M_i)_H \Delta H_i \qquad (4)$$

where M_i and M_{i+1} are the magnetizations measured in field H at temperatures T_i and T_{i+1}, respectively.

The temperature and field dependences of the magnetic entropy change are plotted in Fig. 12. Moderate ΔS_M values are shown around the Curie temperature. The ΔS_M vs T shows an asymmetric form.

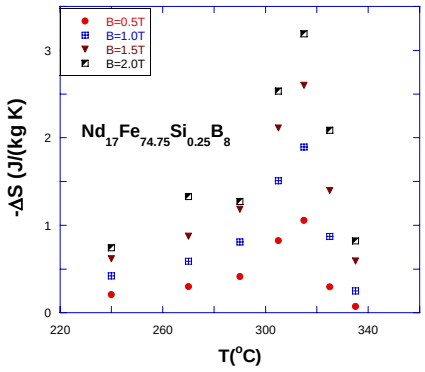

Fig. 12. The entropy changes in $Nd_{15}Fe_{74}Si_1B_8$..

4. Sm-Fe-Si-C alloys

In R-Fe system, no presence of hexagonal $CaCu_5$ type structure was shown [1]. In the R-Co system, although $CaCu_5$ type structure is present, deviations from 1/5 stoichiometry was shown, described by the formula $R_{1-s}Co_{5-2s}$, where s rare-earth atoms were substituted by s dumbbell pairs [15,16]. The presence of metastable $R_{1-s}Fe_{5+2s}$ phases was also reported [17]. For s=0.22, a $TbCu_7$ type structure can be invoked, while for s=0.36-0.38, a 1/9 stoichiometry was shown. The alloy with this composition has a P6/mmm type structure similar to that of $CaCu_5$–type. If s = 0.33, a single R atom out of three is substituted for by one dumbbell pair and the stoichiometry is 2/17. If dumbbell pairs are randomly distributed, the structure is hexagonal. The P6/mmm type structure changes to a rhombohedral $R\bar{3}m$ type through an ordering process of atoms when increasing annealing temperature.In $Sm_{1-s}Fe_{5-2s}$ system, the 3g sites are not affected by the variation of s values. The 2c site of $CaCu_5$ – type structure would transform into Fe(2l) for $s \geq 0.33$.

The $SmFe_{9-y}Si_yC_z$ alloys with $y \leq 1$ were prepared by high energy ball milling and annealing at 650-850 °C [17,18]. The alloys are nanocrystalline, with grain sizes 22-30 nm. The P6/mmm–type structure changes to a rhombohedral one, of $R\bar{3}m$ -type when increasing annealing temperature. The alloys then were carbonated. The corresponding composition was z = 1.

The composition dependences of the Curie temperatures, T_c, in $Sm_2Fe_{17-x}Si_xC_z$ (z=0,2) and $SmFe_{9-y}Si_yC_z$ (z=0,1) alloys are plotted in Fig.13 [17-19]. The T_c values of noncarbonated samples increase gradually when increasing Si content for both systems, although the Curie temperatures of 1/9 phases are higher. The increase of the Curie temperatures can be attributed to the diminution of antiferromagnetic exchange interactions, due to a slight increase of Fe-Fe distances, concomitant with the filling of Fe d band by Si p electrons, implying a shift to a strong ferromagnetic behaviour. In the $Sm_2Fe_{17-x}Si_x$ alloys, crystallizing in $R\bar{3}m$ structure, Si replaces Fe in the 18h sites, while the distances Fe(c)-Fe(c) and Fe(d)-Fe(f) increase, but remain just below 2.50 Å.

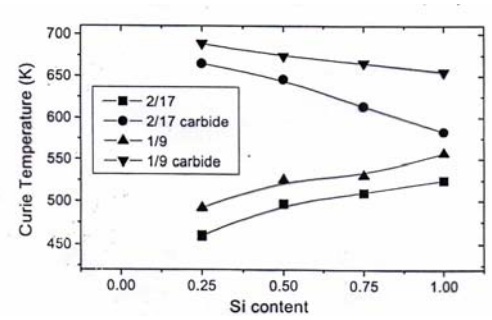

Fig. 13. Composition dependences of the Curie temperatures in $SmFe_{9-y}Si_yC_z$ (z=0, 1) and $Sm_2Fe_{17-x}Si_xC_z$ alloys with z = 0 or 2.

The Curie temperatures of the carbonated samples are sensitively higher than those in noncarbonated ones. Due to the increase of the lattice parameters, as results of the presence of interstitial carbon, the distances between iron atoms are larger than 2.50 Å. This leads to the decrease or cancellation of contributions of the negative exchange interactions between iron pairs. When substituting Fe by Si, in carbonated samples, a decrease of the T_C values was shown, due to dilution effects, as well as of hybridization effects of Fe(3d) bands with Si(p) and C(p) bands.

As results of carbonation, both $Sm_2Fe_{17-x}Si_xC_2$ and $SmFe_{9-y}Si_yC$ systems show uniaxial anisotropy, being thus of interest for technical applications. High coercivities were obtained in metastable $SmFe_{9-y}Si_yC$ nanocrytalline alloys, annealed between 700 and 800 °C [17]. Some hysteresis loops are shown in Fig.14. The coercive fields decrease when decreasing or increasing the annealing temperature outside the above mentioned temperature range. Coercive field of H_c = 13 kOe was obtained in case of sample having y = 0.50 and grain sizes around 22 nm or 15 kOe in nanocrystalline $SmFe_{8.75}Si_{0.25}C$ alloy. The highest coercivities of mechanically alloyed and carbonated samples originate from the presence of the 1/9 metastable hexagonal phase.

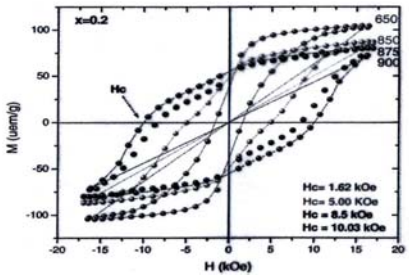

Fig. 14. Hysteresis loops of some $SmFe_{9-y}Si_yC$ alloys [17].

5. Nd-Fe-Co-B hard magnetic phase

The anisotropy fields of $Nd_2Fe_{14-x}Al_xB$ hard magnetic phase increases up to x = 0.5 when iron was substituted by aluminium–Fig.8. In addition, aluminum improve the microstructure, causing an increase of the coercive fieds [20]. When iron is substituted by cobalt, the anisotropy

fields decrease gradually while the Curie temperatures increase. Consequently, it is expected that replacing iron, in $R_2Fe_{14}B$ compounds, by both cobalt and aluminum can be obtained hard magnetic phases having both higher Curie temperatures and anisotropy fields than those of the parent compounds.

The $R_2Fe_{14-x-y}Co_xAl_yB$ with R = Pr or Nd [21] were prepared by melting the constituents in induction furnace and annealing the samples. The composition dependences of the Curie temperatures are plotted in Fig. 15. For constant aluminum content, the T_c values increase when increasing cobalt content. The decrease of the Curie temperatures, due to the presence of aluminum (≅ 70 K/substituted atom) is compensated by the higher increase due to presence of cobalt.

The addition of small quantity of aluminum increases the anisotropy fields – Fig. 16. For constant aluminum content, the anisotropy fields decrease, when increasing cobalt content.

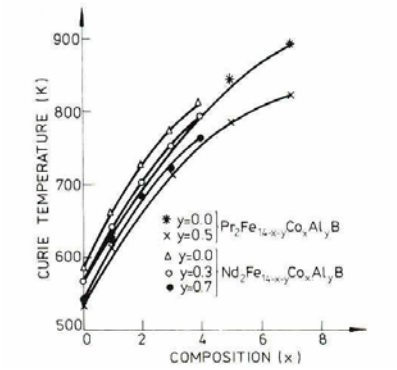

Fig. 15. Composition dependences of the Curie temperatures of $R_2Fe_{14-x-y}Co_xAl_yB$ with R = Nd,Pr.

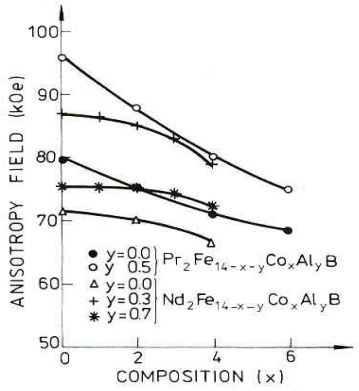

Fig. 16. Composition dependences of the anisotropy fields in $R_2Fe_{14-x-y}Co_xAl_yB$ alloys with R = Nd,Pr.

Thus, the simultaneous substitution of iron by both cobalt and aluminum in $R_2Fe_{14}B$ – based alloys (R = Pr,Nd), in convenable proportions, can increase both the Curie temperatures and anisotropy fields. The saturation magnetizations at, 4.2 K, are somewhat smaller than those of the parent compounds.

6. Sm(Co,Fe,Cu,Zr)$_z$ magnets

The Sm(Co,Fe,Cu,Zr)$_z$ magnets are based mainly on 2/17 phase and consequently have high Curie temperatures and small reversible coefficients of induction and coercive field. Consequently, can be used in devices working at relatively high temperatures [22].

The $Sm(Co_{0.676}Fe_{0.212}Cu_{0.1}Zr_{0.012})_{7.4}$ (sample A) and $Sm(Co_{0.66}Fe_{0.20}Cu_{0.123}Zr_{0.017})_{8.3}$ (sample B) were prepared by melting the constituent elements in an induction furnace. The samples were crushed and powdered by milling. The mean dimensions of powders were (3-4) μm. The powders were oriented in a magnetic field of 30 kOe and pressed at 4 t/cm^2. The samples were sintered at 1170 ^{o}C, followed by a solution treatment at 1150 ^{o}C, during 4 hrs. After rapid cooling, the coercive fields of the alloys were smaller than 0.8 kOe. The samples were multistep annealed under argon atmosphere. After keeping 2 h at 800 ^{o}C, these were maintained at 700 ^{o}C, 600 ^{o}C and 500 ^{o}C during 1h and at 400 ^{o}C, 2h. After this thermal treatment, great changes in the magnetic properties were shown – Fig. 17.

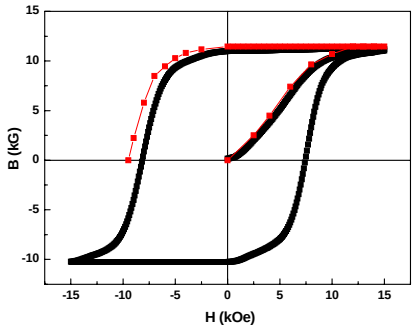

Fig. 17. Hysteresis loops of $Sm(Co_{0.676}Fe_{0.212}Cu_{0.1}Zr_{0.012})_{7.64}$ and $Sm(Co_{0.66}Fe_{0.20}Cu_{0.123}Zr_{0.017})_{8.3}$ alloys.

The first magnetization curve, at room temperature, shows that the coercivity mechanism is determined by pinning of domain walls. The pinning centers are the 1/5 phase, present at the grain boundaries of the 2:17 one. The coercive fields were 9.5 kOe (sample A) and 8.2 kOe (sample B). The remanent inductions and maximum energy products were 11.45 kG, 26.7 MGOe (sample A) and 10 kG and 21 MGOe (sample B). The diminution of the coercive field in sample B can be correlated with a smaller content of 1/5 phase in the sample and consequently a diminution of the number of pinning centers. The composition of this sample approaches to that of 2/17 phase.

The Curie temperatures of both magnets were T_c = 1150 ± 20 K. As a result of high Curie temperature, the reversible coefficients of magnetization were ≅ $4\cdot10^{-2}$%/^{o}C.

7. Conclusions

The exchange interactions in R-M or R-M-B alloys having high transition metal content are dominated by short range M3d-M3d ones. The increase of the Curie temperatures in iron based compounds of R_2Fe_{17} and

$R_2Fe_{14}B$ systems were analysed. The R5d band polarizations in due both to intra-atomic 4f-5d and short range 5d-nd exchange interactions.

The permanent magnet properties of Nd-Fe-Si-B, Nd-Fe-Co-Al-B, Sm-Fe-Si-C and $Sm(Co,Fe,Cu,Zr)_z$ systems can be analysed in correlation with compositions and thermal treatment process.

The research were reported by the contract CNCSIS Consortiu 188/15.06.06 (MS-MM).

References

[1] E. Burzo, A. Chelkowski, H. K. Kirchmayr, Landolt-Börnstein Handbuch, Springer Verlag, vol. 19d2 (1990).
[2] E. Burzo, Rep. Progr. Phys. **61**, 1099 (1998).
[3] I. A. Campbell, J. Phys. F.: Metal Phys. **2**, L47 (1972).
[4] D. Givord, R. Lemaire, IEEE Trans. Magn. **10**, 109 (1979).
[5] M. Richter, J. Phys. D: Appl. Phys. 1017 (1998).
[6] O. K. Anderson, Phys. Rev. **B12**, 5060 (1975); O. K. Anderson, O. Jepsen, Phys. Rev. Letters **53**, 2571 (1984).
[7] R. O. Jones, O. Gunnarson, Rev. Mod. Phys. **61**, 689 (1989).
[8] U. von Barth, L. Hedin, J. Phys. C.: Solid State Phys. **5**, 1629 (1972).
[9] D. Givord, H. S. Li, F. Tasset, J. Appl. Phys. **57**, 4100 (1985).
[10] E. Burzo, E. B. Boltich, M. Q. Huang, W. E. Wallace, 8th Proc. Int. Workshop Rare Earth Magnets and their Applications, Dayton, 1985, p. 711.
[11] E. Burzo, E. Oswald, M. Q. Huang, E. Boltich, W. E. Wallace, J. Appl. Phys. **57**, 4109 (1985).
[12] E. Burzo, F. Givord, C. Rend. Acad. Sci. Paris 271B, 1159 (1970)
[13] E. Burzo, L. Chioncel, I. Costina, S. G. Chiuzbaian, J. Phys: Condens. Matter. **18**, 4681(2006); E. Burzo, P. Vlaic, J. Magn. Magn. Mat. 290-291, 599 (2005).
[14] E. Burzo, J. Less Common Met. **77**, 251 (1981); Solid State Commun. **14**, 1295 (1974); J. Solid State Chem. **16**, 257 (1976).
[15] K. H. J. Buschow, A. S. Van der Goot, J. Less Common Met. **14**, 323 (1968).
[16] D. Givord, J. Laforest, J. Schweizer, F. Tasset, J. Appl. Phys. **50**, 2008 (1979).
[17] C. Djega-Mariadassou, L. Bessais, A. Nandra, E. Burzo, Phys. Rev. **B68**, 024406 (2003).
[18] L. Bessais, C. Djega-Mariadassou, A. Nandra, M. D. Appay, E. Burzo, Phys. Rev., Phys. Rev. **B69**, 064402 (2004).
[19] E. Burzo, C. Djega-Mariadassou, J. Optoelectron. Adv. Mater. **9**, 1757 (2007).
[20] M. Zhang, D. Ma, X. Jiang, S. Liu, 8th Int. Workshop on Rare-Earth Magnets and They Applications, Dayton, Ohio, 1985 p.541.
[21] E. Burzo, A. T. Pedziwiatr, W. E. Wallace, Solid State Commun. **65**, 57 (1987); E. Burzo, N. Plugaru, V. Pop, J. Magn. Magn. Mat. **70**, 343 (1987).
[22] K. J. Strnat, Handbook of Magnetic Materials, Ed. K. H. J. Buschow **4**, 131 (1988).

*Corresponding author: burzo@phys.ubbcluj.ro